NJC

PAPER

View Article Online
View Journal | View Issue

Cite this: *New J. Chem.*, 2016, **40**, 3484

Supramolecular encapsulation of benzocaine and its metabolite *para*-aminobenzoic acid by cucurbit[7]uril

Shengke Li,[a] Hang Yin,[a] Gudrun Martinz,[a] Ian W. Wyman,[b] David Bardelang,[c] Donal H. Macartney[b] and Ruibing Wang*[a]

Received (in Montpellier, France) 18th November 2015,
Accepted 10th February 2016

DOI: 10.1039/c5nj03259h

www.rsc.org/njc

An ester-type local anesthetic agent, benzocaine (BZC), and its metabolite, *para*-aminobenzoic acid (PABA), both form 1 : 1 host–guest complexes with cucurbit[7]uril (CB[7]) in aqueous solution and has been observed by ^{1}H NMR, UV-visible spectroscopic titrations (including Job's plot), electrospray ionization (ESI) mass spectrometry, and density functional theory (DFT) molecular modeling. The host–guest binding affinities are $(2.2 \pm 0.2) \times 10^4$ M^{-1} and $(1.5 \pm 0.2) \times 10^4$ M^{-1} for the protonated BZC and PABA, respectively, in acidic solutions. The binding constants decrease by ~100-fold to approximately 300 and 200 M^{-1} for BZC and PABA, respectively, upon deprotonation of these guest molecules in PBS buffered solution (pH = 7.4). However, the encapsulation of these guest molecules by CB[7] only resulted in very moderate pK_a shifts. This supramolecular encapsulation of BZC and PABA could potentially find applications in drug formulation for the purpose of enhancing bio-absorption as well as reducing methemoglobinemia and allergic reactions caused by the derivation of PABA during the metabolism of BZC.

1. Introduction

It is generally believed that synthetic macrocyclic molecules may mimic the non-covalent encapsulation behaviour of enzymes.[1–3] Particularly, a novel family of macrocyclic hosts known as cucurbit[*n*]urils (CB[*n*]s, *n* = 5–8, 10 and 14) has shown remarkable potential in molecular encapsulation and enzymes biomimetics.[4,5] CB[*n*] compounds consist of *n* glycoluril units connected by 2*n* methylene groups, and they possess not only a hydrophobic internal cavity that can encapsulate guest molecules, but also two carbonyl-fringed portals that are good cation receptors. The chemical activity of a guest molecule is often altered upon encapsulation by CB[*n*].[1,6] Among all of the members of the CB[*n*] family, CB[7] (Fig. 1), in particular, has been widely adopted as a promising molecular capsule of drug molecules because of both its good water-solubility and its capacity to encapsulate organic molecules of a wide range of sizes with binding affinities of up to 10^{17} M^{-1}.[7–10] Following the seminal work on the use of CB[7] for the encapsulation of drug molecules,[11,12] numerous reports regarding the encapsulation of bioactive molecules by CB[7] have been published and well-reviewed in recent years.[1,6,7,13] CB[7] encapsulation often leads to improved solubility, chemical stability, and therapeutic efficacy as well as reduced side effects. Our research groups have investigated the biocompatibility[14] of CB[7] and its complexation with a variety of drug molecules and medically important molecules during the past decade, which have included imidazolium- and thiazolium-based model drugs,[15,16] ranitidine,[17] coumarin,[18] vitamin B_{12} and its coenzyme,[19] and MPTP/MPP$^+$.[20] Very recently, we reported the inclusion of a general anesthetic tricaine for fish by CB[7] and evaluated its biological effects *in vivo*.[21] As a synthetic receptor, CB[7] accelerated the recovery of anesthetized zebrafish by encapsulating tricaine *in vivo*.[21] We recently extended our efforts to study the CB[7] encapsulation of another well-known

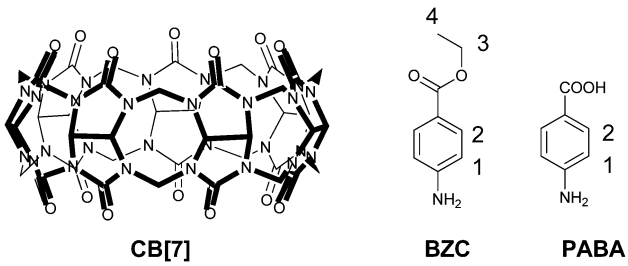

Fig. 1 Molecular structures of CB[7] and the two guest molecules, BZC and PABA. The protons of BZC and PABA molecules are numerically labelled.

[a] State Key Laboratory of Quality Research in Chinese Medicine, Institute of Chinese Medical Sciences, University of Macau, Taipa, Macau, China. E-mail: rwang@umac.mo
[b] Department of Chemistry, Queen's University, Kingston, ON, K7L 3N6, Canada
[c] Aix-Marseille Université, CNRS, Institut de Chimie Radicalaire, UMR 7273, 13013 Marseille, France

structurally relevant anesthetic agent, benzocaine (BZC) (Fig. 1), and its metabolite *para*-aminobenzoic acid (PABA) (Fig. 1).

As an ester-type local anesthetic, BZC is frequently utilized to relieve topical pain and reduce local sensitivity.[22] Due to the low pK_a value of its protonated form, BZC is always present as a neutral species under physiological conditions[23,24] and therefore its corresponding poor solubility in aqueous solution has limited its application in superficial treatments.[25] Additionally, the common problem encountered with local anesthetics is their short duration,[26] and the increasing dosage of BZC in particular often leads to systemic side-effects, as a high concentration of BZC in plasma would be metabolized by esterases generating toxic PABA and its derivatives thus causing methemoglobinemia as well as allergic reactions.[22,27] In order to improve its solubility and bio-availability as well as to decrease the side-effects, various approaches including nanocapsule and liposome delivery formulations have been developed.[25,27–29] In addition to the aforementioned methods, supramolecular encapsulation may also provide a promising pathway toward achieving such a goal, and it has been reported that BZC complexation with cyclodextrin and calixarene derivatives might have this potential.[22,30,31] However, the supramolecular encapsulation of BZC by cucurbit[*n*]urils is yet to be investigated. Our aim is (1) to obtain a clear understanding of the complexation behaviour between CB[7] and BZC as well as its metabolite PABA and (2) to determine the pK_a shifts of BZC and PABA upon binding to the synthetic receptor CB[7]. It is anticipated that such a supramolecular encapsulation may find potential applications in the formulation of this local anesthetic agent for improved delivery with reduced side-effects.

2. Experimental

2.1. Materials

The host molecule CB[7] was prepared according to a literature method.[32] BZC, PABA and PBS pellets were used as received from Sigma-Aldrich. The buffer solutions for the pK_a investigation were prepared by using the buffer pairs of NaOAc/HOAc (0.2 M).

2.2. Instrumentation

The 1D ^{1}H NMR spectra were recorded using a BRUKER ULTRA SHIELD 400 PLUS NMR spectrometer. Meanwhile, the ESI-MS spectra were acquired using THERMO LTQ ORBITRAP XL equipped with an ESI/APcI multiprobe. The UV-visible spectra were all acquired on a HACH DR6000 UV-visible spectrometer using quartz cells with a 1.0 cm path length. The modelled structures of the host–guest complexes involved in this investigation were calculated by energy-minimizations using DFT (B3LYP/6-31G(d)) level of theory using the Gaussian09 Rev. D01 package program, performed at the computing facility of Aix-Marseille Université.

2.3. Preparation of solutions of the complexes

In order to prepare solutions for ^{1}H NMR characterization, a 1 mM solution of BZC and PABA in a D_2O/DCl solution (with a pD of $\sim$2.0) was simply mixed with various amounts of CB[7] without changing the BZC and PABA concentrations. The solutions were sonicated for 3 min before they were characterized using ^{1}H NMR spectroscopy.

In order to perform the UV-visible spectroscopic titrations to determine the binding constant, aqueous solutions of BZC (or PABA) were prepared in PBS buffer solution (pH = 7.4) and acidic solution of HCl (pH = 2). These BZC (or PABA) solutions were subsequently titrated with various volumes of solutions containing the same concentration BZC (or PABA) and an excess of CB[7] to achieve different ratios of BZC (or PABA) : CB[7], while allowing the BZC (or PABA) concentration to remain constant during the entire titration.

In order to prepare solutions for continuous variation titrations for Job's plot, solutions with the appropriate total concentrations of BZC (or PABA) and CB[7] were prepared. Among these solutions, the ratio of CB[7]/([Guest] + CB[7]) was varied from 0 to 1.0 in steps of 0.1.

In order to conduct pH-dependent UV-visible titration for the determination of pK_a values, 0.2 M solutions of NaOAc and HOAc were prepared, and a total of 10 mL of buffer solution with different volumes of the two solutions was utilized to dilute a certain amount of BZC (or PABA) in the absence and in the presence of a large excess of CB[7], with pH values range from 2.5 to 5.8. The solutions with pH values lower than 2.5 were prepared by the direct dilution of a concentrated HCl solution.

3. Results and discussion

By following the experimental methods described above, the host–guest binding behaviours of CB[7] with BZC and PABA were examined, respectively, in detail, and the pK_a shifts of both these guest molecules upon encapsulation by CB[7] were also determined *via* UV-vis spectroscopic titrations under various pH conditions.

3.1. Host–guest binding behaviour study

3.1.1. Binding sites of host–guest complexes. The binding sites of the host–guest complexes can be deduced *via* the complexation-induced shifts (CIS, $\Delta\delta = \delta_{bound} - \delta_{free}$) of the guest proton resonances on the ^{1}H NMR spectra.[17] A CIS value of <0 indicates that the guest protons are shielded due to encapsulation within the non-polar cavity of CB[*n*]. Meanwhile, a CIS value of >0 indicates that the guest protons are located outside of the cavity, but are adjacent to the carbonyl-lined portals of CB[*n*] due to the deshielding effect of the carbonyl groups. A value of CIS = 0 is usually indicative of the guest protons located outside of the cavity and far from the carbonyl-lined portals. As illustrated in Fig. 2a, in a D_2O/DCl solution at pD = 2, the resonances of the two aromatic protons (H(1) and H(2) protons) of the benzene ring and the ethyl protons (H(3) and H(4) protons) of BZC in the presence of an increasing quantity of CB[7] have shifted upfield from those of the free guest, indicating that the entire BZC molecule is situated within the cavity of CB[7]. In particular, the H(1) and H(2) protons have larger CIS values than H(3) and H(4), implying

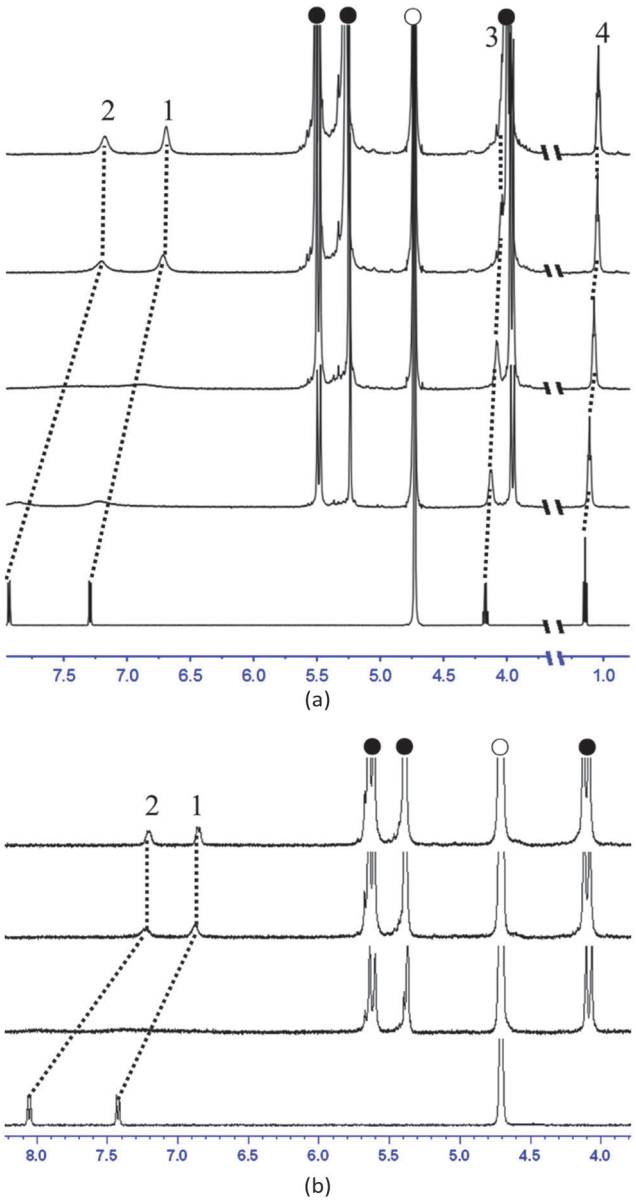

Fig. 2 (a) The ^{1}H NMR titration spectra of BZC (1 mM) in the presence of increasing amounts (0, 0.5, 1.2, 2.2, and 3.1 equiv.) of CB[7] at pD = 2; (b) the ^{1}H NMR titration spectra of PABA (1 mM) in the presence of increasing amounts (0, 0.7, 1.5, and 3.0 equiv.) of CB[7] at pD = 2. The peaks labelled as (●) and (○) are CB[7] and HOD protons, respectively.

that the benzene ring is located in the centre of the cavity and the ethyl group is not encapsulated within the cavity, or possibly that the CB[7] is shuttling between the two groups but encapsulating the benzene ring for the majority of the time. In addition, with increasing amounts of CB[7] (*e.g.* from 0.5 to 1.2 equivalents of CB[7]), the encapsulated aromatic protons exhibited a broadening behaviour (and even disappeared due to extreme broadening) on the ^{1}H NMR spectra, indicative of an intermediate exchange rate of complexation–decomplexation processes between the free and bound BZC species on the ^{1}H NMR timescale.[33]

Considering the BZC metabolite PABA (Fig. 2b) in a D_2O solution at pD = 2, the upfield shift of the resonances of the two aromatic protons (H(1) and H(2) protons) on the benzene ring indicates its location inside the cavity of CB[7]. However, the H(1) protons and H(2) protons exhibit different CIS values of 0.55 ppm and 0.85 ppm, respectively, implying that H(2) is situated deeper within the cavity than H(1), which differs slightly from the case of BZC encapsulation. Similar to BZC, the broadened (even disappearing when a limiting amount of CB[7] was added) proton signals that do not exhibit splitting into free and bound species also demonstrate an intermediate exchange rate of complexation–decomplexation processes between the free and bound PABA species on the ^{1}H NMR timescale. Continuous titration of BZC and PABA guests with increasing amounts of CB[7] (up to 3.0 equivalents) did not yield additional CIS values, providing supportive evidence of the exclusive 1 : 1 binding stoichiometry with relatively strong binding affinity.

In addition to ^{1}H NMR titration, the gas-phase structures of the two host–guest complexes, as calculated by virtue of Density Functional Theory (DFT B3LYP/6-31 basis**), were also employed to clearly describe the binding geometry of CB[7] on BZC and PABA molecules, respectively. The molecular modelling provided further evidence of the 1 : 1 host–guest complex formation, as well as a further indication of the guest binding geometries within the host cavity. As demonstrated in Fig. 3 (left), the full encapsulation of PABA within the cavity of CB[7], presumably through the hydrophobic effect, seems to be consistent with the ^{1}H NMR results (Fig. 2). As expected, the cationic ammonium group is situated at one of the two carbonyl-lined portals *via* ion–dipole interactions, further stabilizing the host–guest complexation. In the case of BZC (Fig. 3 right), similar to PABA, the entire aromatic ring of the guest is preferentially encapsulated by the CB[7] cavity, with the cationic ammonium group sitting at the portal, leaving the ethyl group outside of the cavity. This seems to contradict the ^{1}H NMR results, where the ethyl group seems to be shielded by the hydrophobic cavity of CB[7]. This is not surprising, as the ^{1}H NMR results give an average binding geometry in aqueous solution whereas the DFT modelling proposes one single geometry at a minimized

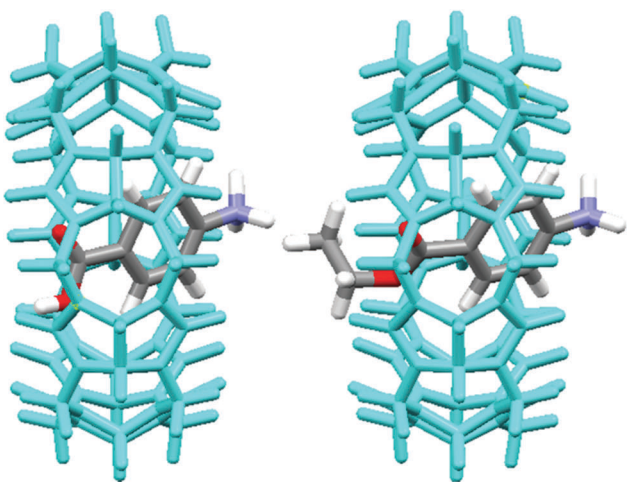

Fig. 3 Energy-minimized structures (DFT/B3LYP/6-31+G(d)** basis set) of PABA@CB[7] (left) and BZC@CB[7] (right).

energy moment. Very likely, the host is shuttling between the ethyl and aromatic groups due to the hydrophobic effect, with the majority of the time being spent with the benzene ring due to the close proximity with the ammonium group. The CB[7] host molecule acts not only as a steric barrier (including the whole aromatic ring) for the guest molecules, but also as a hydrogen bond acceptor for the nitrogen-based proton and hydroxyl protons, by positioning the guests within its cavity to facilitate the optimal hydrogen bonding and cation–dipole interactions.

3.1.2. Binding stoichiometry of host–guest complexes. The 1 : 1 binding stoichiometry has also been confirmed by the continuous variation titration method. For the UV-visible version of this method, the mole fractions of the guest and the host were varied in aqueous solution, while the total concentrations of both the guest and the host were kept constant. If the Job plot exhibits a maximum at 0.5 (the concentration ratio of CB[7] to the sum of the concentrations of CB[7] and the guest), it is indicative of a 1 : 1 binding stoichiometry between the host and the guest.[34,35] The Job plot for the BZC@CB[7] system (with [CB[7]] + [BZC] fixed to 0.05 mM), as monitored using UV-visible spectroscopy (Fig. 4a) at 226 nm, reached a maximum at a ratio of 0.5 for [[CB[7]]/[CB[7]] + [BZC]]. This behaviour thus indicated that the 1 : 1 complexes between CB[7] and BZC represented the dominant species in this concentration range. For PABA, in a similar manner, the peak exhibited a maximum at a ratio of 0.5 at 232 nm for [[CB[7]]/[CB[7]] + [PABA]] (with [CB[7]] + [PABA] fixed to 0.2 mM), demonstrating the formation of 1 : 1 complexes between CB[7] and PABA (Fig. 4b).

Additionally, ESI-MS was performed to further verify the formation of the 1 : 1 host–guest complexes as well, as this method is often considered to provide direct evidence of the binding stoichiometry. As was expected, the ionized host–guest complex between CB[7] and BZC was detected, and the singly charged *m*/*z* peak (experimental *m*/*z* = 1328.4359) corresponds to a 1 : 1 binding ratio, conforming to the calculated *m*/*z* value of 1328.4303. Similarly, the ESI-MS spectrum of the PABA@CB[7] complex also showed a singly charged peak with a *m*/*z* value of 1300.3981, indicative of a 1 : 1 binding ratio and consistent with the calculated *m*/*z* value of 1300.3990.

3.1.3. Binding constants of host–guest complexes. The binding constant of a host–guest complex is often considered as a vital parameter to evaluate the non-covalent binding strength between the host and the guest molecules. Since the pK_a value of the amino group in the electron-deficient aromatic ring of BZC and PABA is less than 2.5,[36,37] the predominantly neutral species in PBS buffered solution (pH = 7.4) would bind differently from the protonated form in acidic solutions (pH = 2) when it comes to complexation with CB[7], thus resulting in a different binding affinity. For both BZC and PABA, the binding constants were thoroughly monitored in both PBS buffered solution (pH = 7.4) and acidic solution (pH = 2) by UV-visible spectroscopy. The UV-visible absorbance spectrum of the neutral BZC at pH = 7.4 exhibited an absorption peak at 285 nm ($\varepsilon \sim 1.6 \times 10^4$ M^{-1} cm^{-1}), consistent with the value reported in the literature (Fig. 5a).[31] Upon gradual addition of increasing amounts of CB[7] (up to 30 equivalents) to a solution of 0.04 mM BZC, the absorbance at 285 nm increased. A subtle hypsochromic shift was also observed, conforming to the encapsulation-induced environment change from the bulk surroundings to macrocyclic microenvironments. Due to the relatively low binding affinity between the neutral BZC and CB[7], the linear regression method was employed for the calculation of binding constants in the PBS solutions.[38] The fitting curve of the absorbance reciprocal at 285 nm against the concentration reciprocal is once again in good agreement with a 1 : 1 binding stoichiometry model and provides a binding constant K_a of $\sim$300 M^{-1} (Fig. 5a inset). Under acidic conditions (pH = 2), the absorbance of BZC experienced a very moderate hypsochromic shift and decreased dramatically to nearly 5-fold ($\varepsilon \sim 3.3 \times 10^3$ M^{-1} cm^{-1}) with respect to that observed at neutral pH (Fig. 5b).

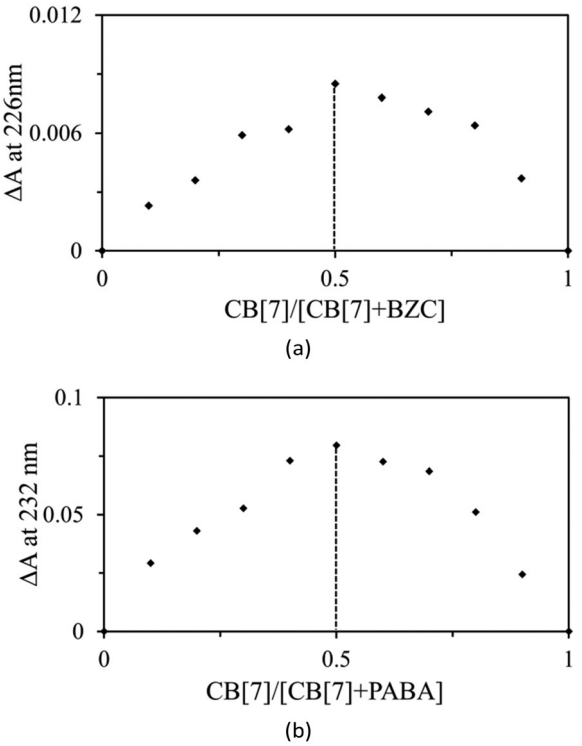

Fig. 4 (a) Job's plot based on a UV-visible continuous variation titration, monitored by the changes in the UV-visible absorbance at 226 nm with [CB[7]] + [BZC] = 0.05 mM in aqueous solution (pH = 2); (b) Job's plot based on a UV-visible continuous variation titration, monitored by the changes in the UV-visible absorbance at 232 nm with [CB[7]] + [PABA] = 0.2 mM in aqueous solution (pH = 2). The maximum exhibited at 0.5 indicates the formation of 1 : 1 complexes between the guest and the host.

After gradual addition of CB[7] to the BZC solution, the absorbance peak of BZC at 278 nm decreased further, along with a modest blue shift in accordance with the encapsulation of the protonated BZC inside of the cavity of CB[7] facing a macrocyclic microenvironment that is different from that of the bulk surroundings. The plot of the absorbance of BZC at 278 nm as a function of the CB[7] concentration in acidic solution (pH = 2) exhibited a non-linear least-squares fit, which is consistent with the previously discussed 1 : 1 binding stoichiometry model (Fig. 5b inset), with a binding constant of K_a = $2.2 \pm 0.2 \times 10^4$ M^{-1}. Such a dramatic difference in the binding

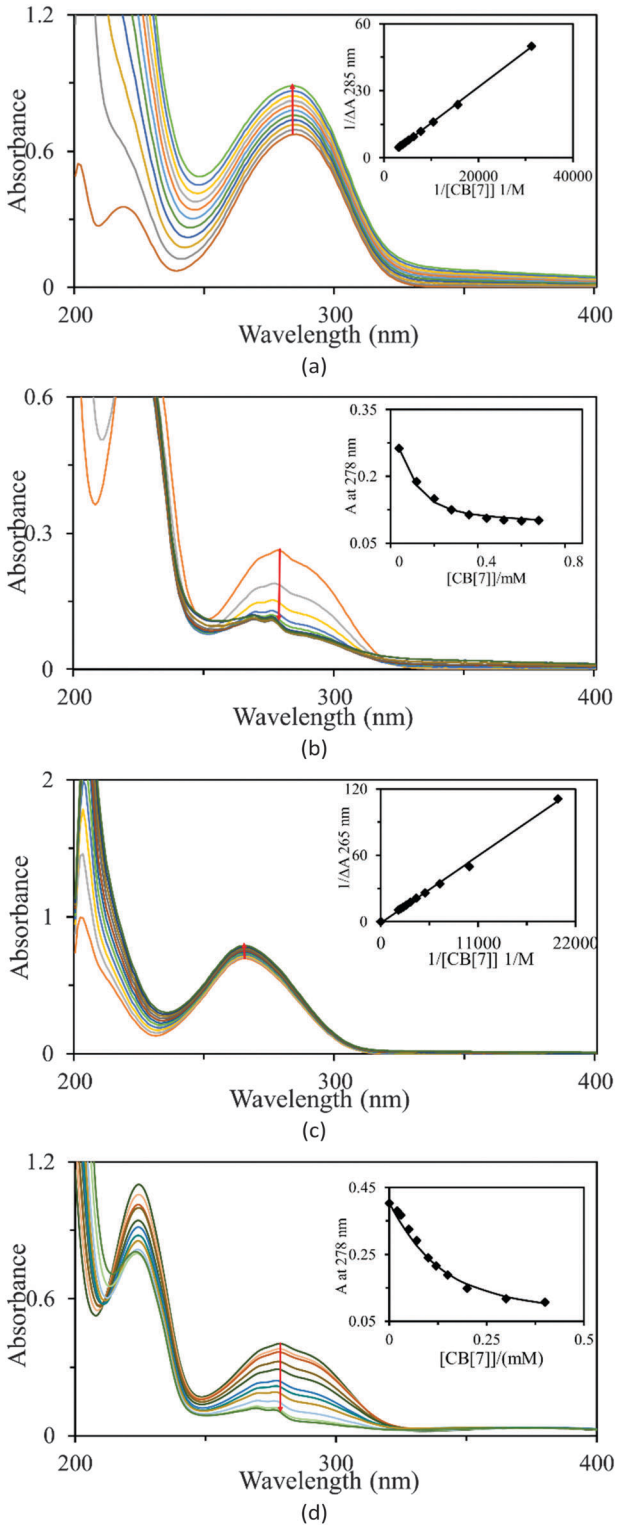

Fig. 5 UV-vis titration of BZC (0.04 mM) in PBS buffer (pH = 7.4) (a), and BZC (0.08 mM) in HCl solutions (pH = 2) (b), with increasing amounts of CB[7]. UV-vis titration of PABA (0.05 mM) in PBS buffer (pH = 7.4) (c) and PABA (0.10 mM) in HCl solution (pH = 2) (d), with increasing amounts of CB[7]. The insets in the four figures show the best fit between experimental points and a 1 : 1 binding model affording a binding constant K_a of $\sim$300 M^{-1}, 2.2 $\pm$ 0.2 $\times$ 10^4 M^{-1}, 200 M^{-1} and 1.5 $\pm$ 0.2 $\times$ 10^4 M^{-1} respectively.

affinities between BZC@CB[7] and BZCH@CB[7] is likely attributed to the ion–dipole interaction between the protonated nitrogen and the carbonyl portal of CB[7]. Additionally, the presence of sodium cations in the PBS solution may have had some negative effects on the binding strength between the neutral BZC and CB[7].[39]

In both PBS buffered solution and acidic solution (pH = 2), PABA@CB[7], the binding behaviours were found to be similar to those of BZC-CB[7] (Fig. 5c and d). The binding constants K_a of PABA and protonated PABA with CB[7] were $\sim$200 and 1.5 $\pm$ 0.2 $\times$ 10^4 M^{-1}, respectively.

3.2. CB[7]-induced pK_a shifts

The two carbonyl-fringed portals of CB[7] are considered as cation receptors that may preferentially bind to cationic species such as protonated amines, thus the pK_a values of the guest molecules often shift upwards upon encapsulation by CB[7].[1] With a thorough understanding of the binding behaviours between CB[7] and the two guest molecules of BZC and PABA, the effect of the inclusion of CB[7] on the pK_a values of the two guest molecules was investigated by a pH titration method *via* UV spectroscopic measurements.[17] The absorbance changes of the guest or the guest–host complexes were monitored with varying pH in aqueous solutions. In particular, the pK_a values of both BZC and PABA were examined in the absence and presence of a large excess equivalents of CB[7]. As illustrated in Fig. 6a, from the plot of absorbance of free BZC at 278 nm against a range of pH values, the pK_a of BZC in the absence of CB[7] was determined to be 2.71 $\pm$ 0.03, which is consistent with the literature reported value.[36] From the plot of the absorbance of BZC@CB[7] complexes at 280 nm against a range of pH values (Fig. 6b), the pK_a value of BZC in the presence of CB[7] was determined to be 2.80 $\pm$ 0.04, which is shifted negligibly (only $\sim$0.1 pK_a unit) from that of the free BZC compound. This extremely negligible pK_a shift may be ascribed to the shuttling of CB[7] between the benzene and ethyl groups of BZC, as discussed previously, thus resulting in less influential interactions on the cationic amino group of BZC.

With regards to PABA, the pH dependent absorbance in the presence and absence of CB[7] showed similar phenomena to that of BZC. As shown in Fig. 6c and d, the pK_a of PABA in the absence of CB[7] is 2.63 $\pm$ 0.03, which is consistent with the reported result,[37] while the pK_a in the presence of a large excess of CB[7] shifted to 3.12 $\pm$ 0.07 (approximately 0.5 pK_a units). Such a pK_a shift of PABA is more pronounced than that of BZC, which may be attributed to the full encapsulation of PABA within the cavity of CB[7], thus optimizing the electrostatic interactions and hydrogen bonding interactions between the host carbonyl portal and the guest cationic amino group.

Although it has been recognized that a cation-receptor driven pK_a shift is difficult to predict, theoretically the large differences ($\sim$100-fold) of binding affinities (K_a), between the protonated and deprotonated host–guest species, might result in approximately a 2 pK_a unit shift.[1] However, the binding strength differences observed in this study might be a result of the different mediums, as it has been known that competitive salts (*e.g.* sodium salt in buffer) may intervene CB[*n*] based on

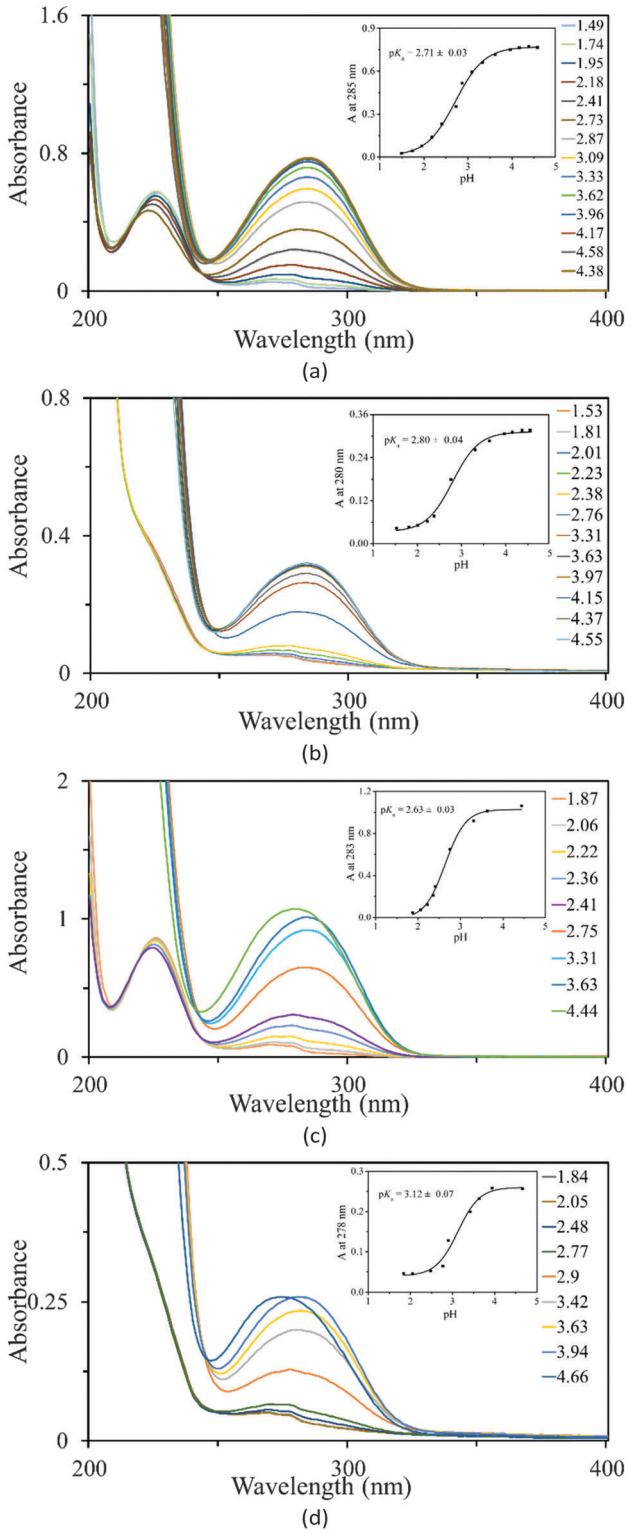

Fig. 6 Plots of pH-dependent UV-visible titrations for determining pK_a values of BZC and PABA in the absence and presence of 20 equivalents of CB[7]; (a) BZC; (b) BZC with CB[7]; (c) PABA; and (d) PABA with CB[7]. The concentration of each guest is ~0.1 mM. The insets in these figures show the best fits of absorbance against pH per sigmoidal function, affording corresponding pK_a values in these systems.

the host–guest complexation.[39] On the other hand, the medium was consistently acetate buffered during pH titrations, rendering reliable determinations of pK_a values and the associated pK_a shifts.

4. Conclusions

In summary, we have investigated the host–guest binding behaviours of benzocaine and its metabolite *para*-aminobenzoic acid with cucurbit[7]uril in aqueous solution at different pH values. The protonated guests formed relatively tight host–guest complexes with binding affinities in the order of 10^4 M^{-1}. Conversely, the binding affinities decrease by ~100-fold when the guest molecules are in their neutral forms, in comparison with those of the corresponding protonated forms in notably different media. Upon encapsulation by cucurbit[7]uril, benzocaine showed a negligible pK_a shift, while *para*-aminobenzoic acid exhibited a moderate pK_a shift of 0.5 units. The benzocaine and *para*-aminobenzoic acid supramolecular complexation with cucurbit[7]uril may have potential applications in the development of benzocaine-based drug formulations, drug delivery, as well as the minimization of benzocaine's side effects induced by *para*-aminobenzoic acid through supramolecular encapsulation in plasma. We are currently working along this line of research.

Acknowledgements

The University of Macau Research Fund (SRG2014-00025), Macau Science and Technology Development Fund (FDCT/020/2015/A1) and the Natural Sciences and Engineering Research Council Grant (NSERC, Canada) are gratefully acknowledged for providing financial support.

Notes and references

1 I. Ghosh and W. M. Nau, *Adv. Drug Delivery Rev.*, 2012, **64**, 764–783.
2 B. Honig and A. Nicholls, *Science*, 1995, **268**, 1144–1149.
3 C. S. Mahon and D. A. Fulton, *Nat. Chem.*, 2014, **6**, 665–672.
4 L. Zheng, S. Sonzini, M. Ambarwati, E. Rosta, O. A. Scherman and A. Herrmann, *Angew. Chem., Int. Ed.*, 2015, **54**, 13007–13011.
5 Y. Jang, R. Natarajan, Y. H. Ko and K. Kim, *Angew. Chem., Int. Ed. Engl.*, 2014, **53**, 1003–1007.
6 D. H. Macartney, *Isr. J. Chem.*, 2011, **51**, 600–615.
7 D. Shetty, J. K. Khedkar, K. M. Park and K. Kim, *Chem. Soc. Rev.*, 2015, **44**, 8747–8761.
8 E. Masson, X. Ling, R. Joseph, L. Kyeremeh-Mensah and X. Lu, *RSC Adv.*, 2012, **2**, 1213–1247.
9 K. I. Assaf and W. M. Nau, *Chem. Soc. Rev.*, 2015, **44**, 394–418.
10 L. Cao, M. Sekutor, P. Y. Zavalij, K. Mlinaric-Majerski, R. Glaser and L. Isaacs, *Angew. Chem., Int. Ed. Engl.*, 2014, **53**, 988–993.
11 Y. J. Jeon, S. Y. Kim, Y. H. Ko, S. Sakamoto, K. Yamaguchi and K. Kim, *Org. Biomol. Chem.*, 2005, **3**, 2122–2125.

12 N. J. Wheate, A. I. Day, R. J. Blanch, A. P. Arnold, C. Cullinane and J. G. Collins, *Chem. Commun.*, 2004, 1424–1425.
13 S. Walker, R. Oun, F. J. McInnes and N. J. Wheate, *Isr. J. Chem.*, 2011, **51**, 616–624.
14 H. Chen, J. Y. W. Chan, X. Yang, I. W. Wyman, D. Bardelang, D. H. Macartney, S. M. Y. Lee and R. Wang, *RSC Adv.*, 2015, **5**, 30067–30074.
15 R. Wang, L. Yuan and D. H. Macartney, *Chem. Commun.*, 2006, 2908–2910.
16 S. Li, X. Miao, I. W. Wyman, Y. Li, Y. Zheng, Y. Wang, D. H. Macartney and R. Wang, *RSC Adv.*, 2015, **5**, 56110–56115.
17 R. Wang and D. H. Macartney, *Org. Biomol. Chem.*, 2008, **6**, 1955–1960.
18 X. Miao, Y. Li, I. Wyman, S. M. Y. Lee, D. H. Macartney, Y. Zheng and R. Wang, *Med. Chem. Commun.*, 2015, **6**, 1370–1374.
19 R. Wang, B. C. Macgillivray and D. H. Macartney, *Dalton Trans.*, 2009, 3584–3589.
20 S. Li, H. Chen, X. Yang, D. Bardelang, I. W. Wyman, J. Wan, S. M. Y. Lee and R. Wang, *ACS Med. Chem. Lett.*, 2015, **6**, 1174–1178.
21 H. Chen, J. Y. W. Chan, S. Li, J. J. Liu, I. W. Wyman, S. M. Y. Lee, D. H. Macartney and R. Wang, *RSC Adv.*, 2015, **5**, 63745–63752.
22 L. M. Pinto, L. F. Fraceto, M. H. Santana, T. A. Pertinhez, S. O. Junior and E. de Paula, *J. Pharm. Biomed. Anal.*, 2005, **39**, 956–963.
23 S. Li and D. Li, *Spectrochim. Acta, Part A*, 2011, **82**, 396–405.
24 R. D. Porasso, W. F. Bennett, S. D. Oliveira-Costa and J. J. Lopez Cascales, *J. Phys. Chem. B*, 2009, **113**, 9988–9994.
25 N. F. De Melo, D. R. De Araujo, R. Grillo, C. M. Moraes, A. P. De Matos, E. de Paula, A. H. Rosa and L. F. Fraceto, *J. Pharm. Sci.*, 2012, **101**, 1157–1165.
26 C. M. Moraes, A. P. de Matos, E. de Paula, A. H. Rosa and L. F. Fraceto, *Mater. Sci. Eng., B*, 2009, **165**, 243–246.
27 N. F. de Melo, R. Grillo, V. A. Guilherme, D. R. de Araujo, E. de Paula, A. H. Rosa and L. F. Fraceto, *Pharm. Res.*, 2011, **28**, 1984–1994.
28 P. Mura, F. Maestrelli, M. L. Gonzalez-Rodriguez, I. Michelacci, C. Ghelardini and A. M. Rabasco, *Eur. J. Pharm. Biopharm.*, 2007, **67**, 86–95.
29 C. Puglia, M. G. Sarpietro, F. Bonina, F. Castelli, M. Zammataro and S. Chiechio, *J. Pharm. Sci.*, 2011, **100**, 1892–1899.
30 L. M. Arantes, E. V. Varejao, K. J. Pelizzaro-Rocha, C. M. Cereda, E. de Paula, M. P. Lourenco, H. A. Duarte and S. A. Fernandes, *Chem. Biol. Drug Des.*, 2014, **83**, 550–559.
31 E. Iglesias, *Photochem. Photobiol. Sci.*, 2011, **10**, 531–542.
32 A. Day, A. P. Arnold, R. J. Blanch and B. Snushall, *J. Org. Chem.*, 2001, **66**, 8094–8100.
33 R. Wang, D. Bardelang, M. Waite, K. A. Udachin, D. M. Leek, K. Yu, C. I. Ratcliffe and J. A. Ripmeester, *Org. Biomol. Chem.*, 2009, **7**, 2435–2439.
34 K. Hirose, *J. Inclusion Phenom. Macrocyclic Chem.*, 2001, **39**, 193–209.
35 J. S. Renny, L. L. Tomasevich, E. H. Tallmadge and D. B. Collum, *Angew. Chem., Int. Ed.*, 2013, **52**, 11998–12013.
36 J. Bezencon, M. B. Wittwer, B. Cutting, M. Smiesko, B. Wagner, M. Kansy and B. Ernst, *J. Pharm. Biomed. Anal.*, 2014, **93**, 147–155.
37 S. Shaomin, Y. Yu and P. Jinghao, *Anal. Chim. Acta*, 2002, **458**, 305–310.
38 P. Thordarson, *Chem. Soc. Rev.*, 2011, **40**, 1305–1323.
39 W. Ong and A. E. Kaifer, *J. Org. Chem.*, 2004, **69**, 1383–1385.

